EFFECT OF LOW FREQUENCY SIGNAL UP-CONVERSION ON FREQUENCY STABILITY IN CAPACITIVELY TRANSDUCED MICRORESONATORS

James M.L. Miller^{1,*}, Nicholas E. Bousse², Hyun-Keun Kwon³, Gabrielle D. Vukasin⁴, Steven W. Shaw^{5,6}, and Thomas W. Kenny²

¹Trine University, Angola, Indiana 46703, USA

²Stanford University, Stanford, California 94305, USA

³Apple Incorporated, Cupertino, California 95014, USA

⁴Robert Bosch Research and Technology Center, Sunnyvale, California 94085, USA

⁵Florida Institute of Technology, Melbourne, Florida 32901, USA

⁶Michigan State University, East Lansing, Michigan 48823, USA

ABSTRACT

Low frequency noise (LFN) is ubiquitous in many electronic devices, however its effect on the oscillators and resonant sensors that underlie modern technology is rarely considered. Here we demonstrate LFN up-conversion, or aliasing, in encapsulated microelectromechanical systems (MEMS) resonators measured with a thermomechanical-noise-limited readout. By delineating and mitigating the LFN up-conversion in a set of devices, we improve the frequency stability limit by an order-of-magnitude.

KEYWORDS

MEMS resonator, capacitive transduction, noise aliasing, low frequency noise, frequency stability

INTRODUCTION

Microelectromechanical systems (MEMS) oscillators are gradually replacing quartz-based oscillators as timing references in mobile devices and other applications [1, 2]. The frequency stability of the resonant element is an important consideration for these devices because it impacts the performance of the timing reference. There are several emerging techniques for improving the frequency stability of microelectromechanical systems oscillators by operating in the nonlinear regime of the resonator, such as operating at zero-dispersion points [3, 4], utilizing coupling between modes [5], or increasing the linear operating range [6]. These techniques are promising but have yet to be incorporated into oscillators and resonant sensors fabricated using wafer-scale encapsulation process that forms the basis of commercial devices [7]. Frequency stability can be improved by pushing the oscillator operation into the nonlinear regime if the oscillator noise is limited by the fundamental thermomechanical noise of the resonator and other extrinsic noise mechanisms are not present.

Our development of low-noise capacitive transduction in encapsulated MEMS resonators enables thermomechanical-noise-limited frequency stability at moderate vibration amplitudes [8], but several noise sources conspire to limit the frequency stability at vibration amplitudes approaching the resonator nonlinearity limit. Here we identify and directly mitigate one such noise source: low frequency noise (LFN) upconversion, also known as low frequency noise aliasing [9].

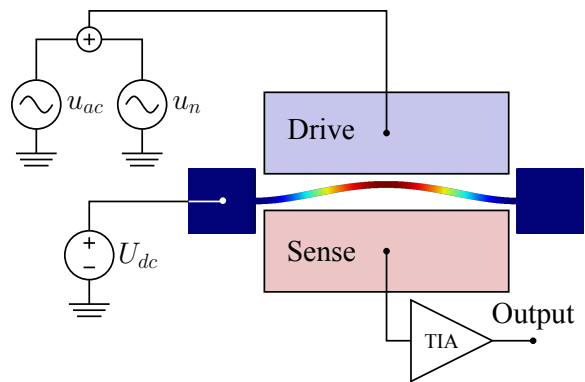


Figure 1: A diagram for the low frequency noise (LFN) voltage noise up-conversion mechanism, as additional voltage noise in the drive electrode line. A harmonic symbol is used to denote LFN because up-conversion can also occur for intentional low frequency harmonic voltages. To track the resonance frequency, we establish a phase-locked loop with a Zurich Instruments (ZI) lock-in amplifier. The beam mode shape and gaps are exaggerated for clarity.

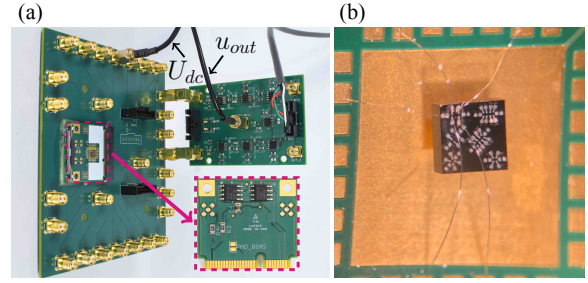


Figure 2: (a) The thermomechanical-noise-limited amplifier setup for capacitive detection of the encapsulated MEMS beam motion. The parasitic noise is minimized by wirebonding the sense electrode directly to the first stage operational amplifier input. (b) A chip containing a device-under-test, suspended off the substrate by the wire-bonds to the drive, sense, and bias voltage electrodes to minimize clamping loss [10].

LFN includes ambient electromagnetic noise such as 60 Hz harmonics and voltage noise introduced by the voltage supply and temperature chamber. We directly mitigate these noise sources by utilizing a battery supply, minimizing the lock-in amplifier drive cable length, and shutting off the temperature chamber.

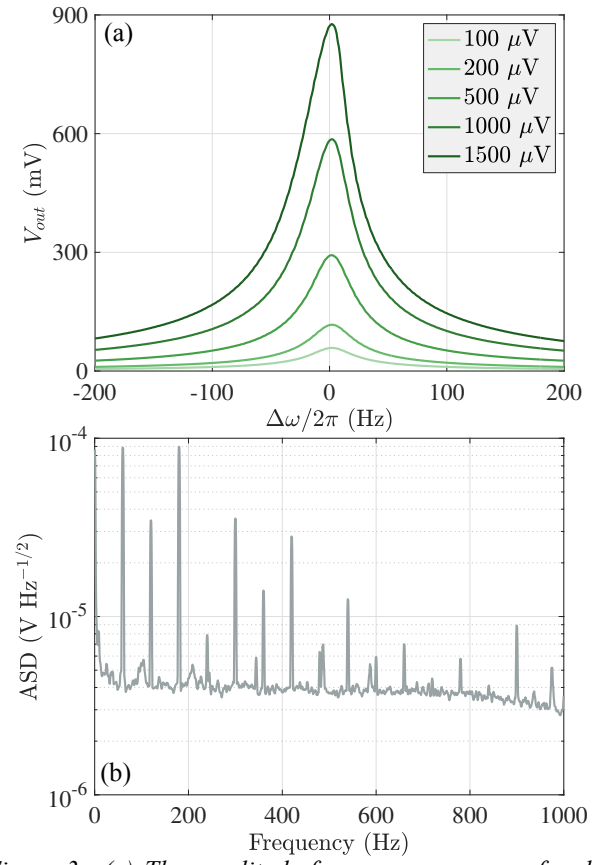


Figure 3: (a) The amplitude-frequency responses for drive voltage amplitudes ranging from $100~\mu V$ to $1500~\mu V$, illustrating the approach to nonlinear behavior. (b) The measured low frequency noise (LFN) spectrum on the transimpedance amplifier (TIA) input while connected to the device sense electrode without noise mitigation, illustrating 60 Hz harmonics.

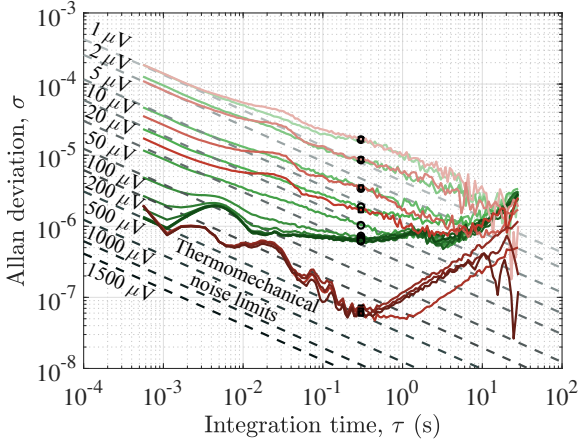


Figure 4: The frequency stability for a device before (green) and after (red) minimizing LFN up-conversion. The Allan deviation of the resonance frequency for varying drive voltage, with the predicted thermomechanical contribution (dashed lines) [11].

MODEL

Low frequency noise at $\Delta\omega$ frequency results in an upconverted current out of the sense electrode at frequencies $\omega\pm$ $\Delta\omega$ with an amplitude given by [9]:

$$i_n = 2(\Gamma_c + \Gamma_{F,Lin} + \Gamma_{F,NL} + \Gamma_k)u_{ac}u_n \tag{1}$$

where the up-conversion of low frequency noise arises from several mechanisms, including current aliasing Γ_c , force aliasing $\Gamma_{F,Lin}$ and $\Gamma_{F,NL}$, and spring aliasing Γ_k following [9].

The current aliasing factor is given by:

$$\Gamma_c = \frac{\omega_0 Q \eta^2}{2k U_{dc}},\tag{2}$$

which arises from the time-varying drive electrode gap capacitance and only requires a linear dependence of capacitance on displacement, e.g. which occurs for a comb drive.

The linear force aliasing factor is given by:

$$\Gamma_{F,Lin} = \frac{\omega_0 Q \eta^2}{2k U_{dc}},\tag{3}$$

which arises from mixing of the drive voltage with the noise voltage in the quadratic capacitive force and only requires a linear dependence of capacitance on displacement.

The nonlinear force aliasing factor is given by:

$$\Gamma_{F,NL} = -\frac{j\omega_0 Q^2 \eta^3}{k^2 d},\tag{4}$$

which arises from mixing of the noise voltage with the DC bias voltage and the vibration amplitude and uses the quadratic dependence of capacitance on displacement, e.g. which occurs for parallel plate capacitance.

The spring aliasing factor is given by:

$$\Gamma_k = \frac{j3\eta^4\omega_0 Q^2 U_{dc}}{2k^3 d^2},\tag{5}$$

which arises from mixing in the nonlinear spring force arising from nonlinearity in the capacitance.

The electromechanical transduction factor η is given by:

$$\eta = U_{dc} \frac{\partial C}{\partial x} \approx \frac{U_{dc} C_0}{d},$$
(6)

where the drive electrode capacitance at zero displacement is given by:

$$C_0 = \frac{\epsilon_0 A_{el}}{d} \tag{7}$$

and where u_{ac} is the amplitude of the drive voltage at near the mode natural frequency $\omega_0,\,u_n$ is the amplitude of the low frequency noise voltage, Q is the quality factor, k is the mode spring constant, U_{dc} is the DC bias voltage, d is the drive electrode capacitive gap size, ϵ_0 is the permittivity of free space, A_{el} is the drive electrode area, and j is an imaginary number.

EXPERIMENT AND DISCUSSION

We demonstrate the influence of LFN aliasing on oscillator frequency stability using the measurement setup in Fig. 2. The characterized devices are doubly clamped beam resonators previously discussed in [8], which are fabricated within

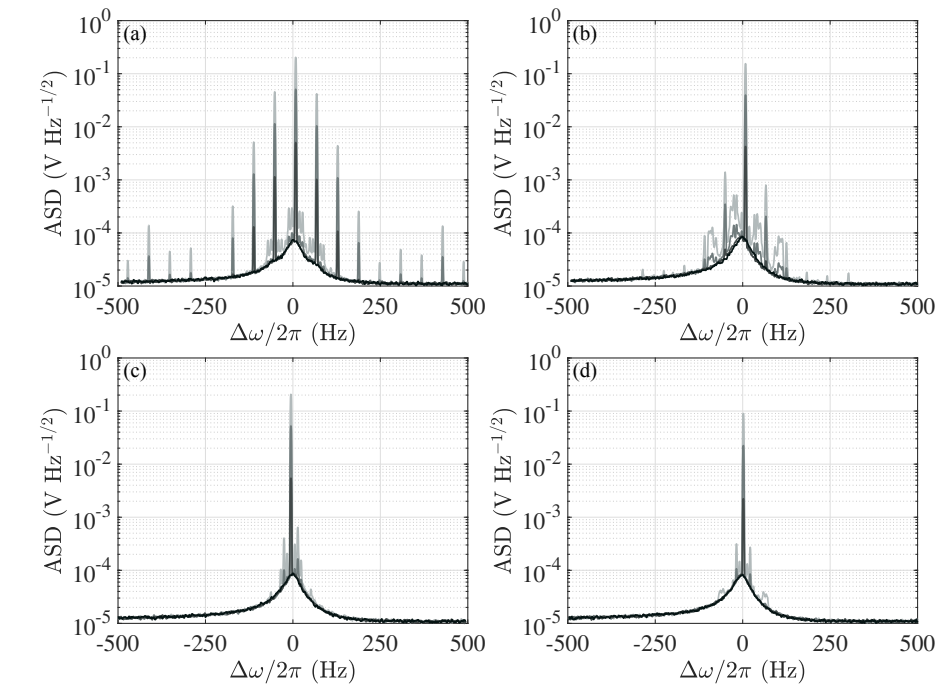


Figure 5: (a) The measured resonance thermomechanical noise spectrum for increasing drive amplitude at resonance ranging from 0 μ V to 400 μ V (dark to light gray), with the oven off and the battery bias supply outside of the oven, illustrating upconverted 60 Hz harmonics LFN. The black spectrum corresponds to the thermomechanical noise without any external drive. (b) The noise spectrum with the battery bias inside the oven and the oven on, illustrating up-converted LFN from the oven. (c) The noise spectrum with the battery supply inside the oven, the oven off, and minimizing drive cable length. (d) The same as (c) except a 3-stage drive high-pass filter is used on the drive.

a wafer-scale encapsulation process which eliminates gas damping and confers excellent long-term frequency stability. These devices are selected for this work because they have nearly the smallest achievable lumped mass for this fabrication technology ($m\!=\!55.15$ ng for the fundamental flexural mode) and strong electromechanical coupling to the drive and sense electrodes, making them highly susceptible to the ambient LFN in Fig. 3(b).

The noise aliasing factors are estimated for this device in Table 1. The current aliasing factor Γ_c and the linear force aliasing factor $\Gamma_{F,Lin}$ holds even for a completely linear capacitive transduction, while the nonlinear force aliasing factor $\Gamma_{F,NL}$ and the spring aliasing factor Γ_k both occur because of nonlinearity in the capacitance. We see that these nonlinear mechanisms are largely responsible for the LFN aliasing in this device, although a fully linear capacitive transduction would still exhibit some LFN aliasing.

The frequency stability for two identical beam devices is measured via the Allan deviation in Fig. 4, with and without LFN up-conversion minimization. At small drive amplitudes, the Allan deviations for the two devices at short timescales agree with each other. At large drive amplitudes, the ADEV for the first device plateaus at the frequency stability imposed by the LFN up-conversion, whereas the ADEV for the second device with LFN mitigation continues to improve.

The effect of LFN up-conversion on the resonator noise spectrum is depicted in Fig. 5, and shows the presence of am-

Table 1: The estimated noise aliasing factors for the doubly clamped beam resonator devices. The assumed bias voltage is $U_{dc} = 11.2$ V, and other device parameter values are delineated in [8].

Noise factor	Value	Description
$ \Gamma_c $	$5.16 \times 10^{-6} \text{ A/V}^2$	Current
$ \Gamma_{F,Lin} $	$5.16 \times 10^{-6} \text{ A/V}^2$	Linear force
$ \Gamma_{F,NL} $	$1.07 \times 10^{-2} \text{ A/V}^2$	Nonlinear force
$ \Gamma_k $	$8.40 \times 10^{-3} \text{ A/V}^2$	Spring

bient LFN arising from 60 Hz harmonics in the cabling and bias voltage supply as well as broadband noise from the temperature-stabilization oven. These noise sources are mitigated at their source by using a battery supply in the oven and turning off the oven. The up-converted noise is further minimized by employing a high-pass filter (HPF) on the drive.

The frequency stability at a 300 ms integration time is plotted versus drive voltage for four comparable beam resonators in Fig. 6. The first three devices (A,B, and C) are operated without LFN mitigation, whereas the fourth device (D) is operated with LFN mitigation. The frequency stability of the device with LFN mitigation tracks the limit imposed by thermomechanical noise until the predicted onset of res-

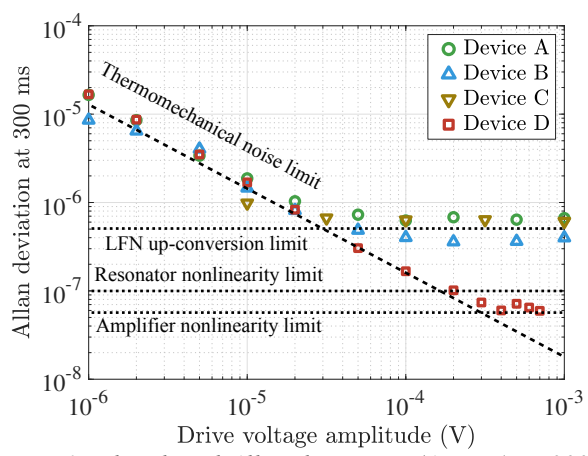


Figure 6: The plotted Allan deviations (ADEVs) at 300 ms integration time versus drive voltage for devices A, B, and C which do not minimize LFN up-conversion, as well as device D after minimizing LFN up-conversion. The LFN up-conversion limit is determined from inspection, and the nonlinear limit to frequency stability is derived for this device from [12].

onator nonlinearity. The frequency stability for device D at large drive amplitudes is limited by the onset of amplifier nonlinearity, which masks the effects arising from intrinsic resonator nonlinearity. Future work will develop an amplifier which maintains thermomechanical-noise-limited resolution while extending the dynamic range, enabling studies of frequency stability in strongly nonlinear encapsulated MEMS resonators.

We identify LFN up-conversion as an important noise mechanism which can limit the frequency stability in MEMS oscillators, and use direct techniques to mitigate the noise, enabling a ten-fold improvement in oscillator frequency stability limit. Alternately, utilizing drive tone mixing [13, 11] or parametric techniques [14] can evade this noise source by avoiding applying a large amplitude capacitive drive tone at resonance.

ACKNOWLEDGMENTS

Fabrication was performed in the nano@Stanford labs, which are supported by the National Science Foundation (NSF) as part of the National Nanotechnology Coordinated Infrastructure under award ECCS-1542152, with support from the Defense Advanced Research Projects Agency Precise Robust Inertial Guidance for Munitions (PRIGM) Program, managed by Ron Polcawich and Robert Lutwak.

REFERENCES

- [1] S. Zaliasl, J. C. Salvia, G. C. Hill, L. W. Chen, K. Joo, R. Palwai, N. Arumugam, M. Phadke, S. Mukherjee, H.-C. Lee, et al., "A 3 ppm 1.5×0.8 mm² 1.0 μA 32.768 kHz MEMS-based oscillator," *IEEE J. Solid-State Circuits*, vol. 50, pp. 291–302, 2015.
- [2] G. Wu, J. Xu, E. J. Ng, and W. Chen, "MEMS resonators for frequency reference and timing applications," *J. Microelectromech. Syst.*, vol. 29, pp. 1137–1166, 2020.

- [3] L. G. Villanueva, E. Kenig, R. B. Karabalin, M. H. Matheny, R. Lifshitz, M. C. Cross, and M. L. Roukes, "Surpassing fundamental limits of oscillators using nonlinear resonators," *Phys. Rev. Lett.*, vol. 110, p. 177208, 2013.
- [4] L. Huang, S. M. Soskin, I. A. Khovanov, R. Mannella, K. Ninios, and H. B. Chan, "Frequency stabilization and noise-induced spectral narrowing in resonators with zero dispersion," *Nat. Commun.*, vol. 10, p. 3930, 2019.
- [5] D. Antonio, D. H. Zanette, and D. López, "Frequency stabilization in nonlinear micromechanical oscillators," *Nat. Commun.*, vol. 3, p. 806, 2012.
- [6] S. K. Roy, V. T. K. Sauer, J. N. Westwood-Bachman, A. Venkatasubramanian, and W. K. Hiebert, "Improving mechanical sensor performance through larger damping," *Science*, vol. 360, p. eaar5220, 2018.
- [7] Y. Yang, E. J. Ng, Y. Chen, I. B. Flader, and T. W. Kenny, "A unified epi-seal process for fabrication of high-stability microelectromechanical devices," *J. Microelectromech. Syst.*, vol. 25, pp. 489–497, 2016.
- [8] J. M. L. Miller, N. E. Bousse, D. B. Heinz, H. J. K. Kim, H.-K. Kwon, G. D. Vukasin, and T. W. Kenny, "Thermomechanical-noise-limited capacitive transduction of encapsulated MEM resonators," *J. Microelectromech. Syst.*, vol. 28, no. 6, pp. 965–976, 2019.
- [9] V. Kaajakari, J. K. Koskinen, and T. Mattila, "Phase noise in capacitively coupled micromechanical oscillators," *IEEE Trans. Ultrason. Ferroelectr. Freq. Control*, vol. 52, pp. 2322–2331, 2005.
- [10] J. M. L. Miller, G. D. Vukasin, Z. Zhang, H.-K. Kwon, A. Majumdar, T. W. Kenny, and S. W. Shaw, "Effects of remote boundary conditions on clamping loss in micromechanical resonators," *J. Microelectromech. Syst.*, vol. 31, pp. 204–216, 2022.
- [11] M. Sansa, E. Sage, E. C. Bullard, M. Gély, T. Alava, E. Colinet, A. K. Naik, L. G. Villanueva, L. Duraffourg, M. L. Roukes, *et al.*, "Frequency fluctuations in silicon nanoresonators," *Nat. Nanotechnol.*, vol. 11, pp. 552–558, 2016.
- [12] H. W. Postma, I. Kozinsky, A. Husain, and M. L. Roukes, "Dynamic range of nanotube-and nanowire-based electromechanical systems," *Appl. Phys. Lett.*, vol. 86, 2005.
- [13] G. Bahl, J. Salvia, H. K. Lee, R. Melamud, B. Kim, R. Howe, and T. Kenny, "Heterodyned electrostatic transduction oscillators evade low frequency noise aliasing," in *Proc. Solid-State Sens. Actuators Microsyst. Workshop*, pp. 6–10, 2010.
- [14] N. E. Bousse, J. M. L. Miller, G. D. Vukasin, H.-K. Kwon, S. W. Shaw, and T. W. Kenny, "Tuning frequency stability in micromechanical resonators with parametric pumping," in *Proc. IEEE Int. Conf. MEMS*, pp. 987–990, IEEE, 2022.

CONTACT

James M.L. Miller; millerj1@trine.edu